TOXICOLOGICAL SCIENCES **101(1)**, 122–131 (2008)
doi:10.1093/toxsci/kfm243
Advance Access publication September 17, 2007

# Inhalation Toxicity and Lung Toxicokinetics of $C_{60}$ Fullerene Nanoparticles and Microparticles

Gregory L. Baker,[1] Amit Gupta, Mark L. Clark, Blandina R. Valenzuela, Lauren M. Staska, Sam J. Harbo, Judy T. Pierce, and Jeffery A. Dill

*Battelle Toxicology Northwest, Richland, Washington 99354*

Received May 7, 2007; accepted August 22, 2007

**While several recent reports have described the toxicity of water-soluble $C_{60}$ fullerene nanoparticles, none have reported the toxicity resulting from the inhalation exposures to $C_{60}$ fullerene nanoparticles or microparticles. To address this knowledge gap, we exposed male rats to $C_{60}$ fullerene nanoparticles (2.22 mg/m$^3$, 55 nm diameter) and microparticles (2.35 mg/m$^3$, 0.93 μm diameter) for 3 h a day, for 10 consecutive days using a nose-only exposure system. Nanoparticles were created utilizing an aerosol vaporization and condensation process. Nanoparticles and microparticles were subjected to high-pressure liquid chromatography (HPLC), XRD, and scanning laser Raman spectroscopy, which cumulatively indicated no chemical modification of the $C_{60}$ fullerenes occurred during the aerosol generation. At necropsy, no gross or microscopic lesions were observed in either group of $C_{60}$ fullerene exposures rats. Hematology and serum chemistry results found statistically significant differences, although small in magnitude, in both exposure groups. Comparisons of bronchoalveolar (BAL) lavage fluid parameters identified a significant increase in protein concentration in rats exposed to $C_{60}$ fullerene nanoparticles. BAL fluid macrophages from both exposure groups contained brown pigments, consistent with $C_{60}$ fullerenes. $C_{60}$ lung particle burdens were greater in nanoparticle-exposed rats than in microparticle-exposed rats. The calculated lung deposition rate and deposition fraction were 41 and 50% greater, respectively, in $C_{60}$ fullerene nanoparticle–exposed group than the $C_{60}$ fullerene microparticle–exposed group. Lung half-lives for $C_{60}$ fullerene nanoparticles and microparticles were 26 and 29 days, respectively. In summary, this first *in vivo* assessment of the toxicity resulting from inhalation exposures to $C_{60}$ fullerene nanoparticles and microparticles found minimal changes in the toxicological endpoints examined. Additional toxicological assessments involving longer duration inhalation exposures are needed to develop a better and more conclusive understanding of the potential toxicity of inhaled $C_{60}$ fullerenes whether in nanoparticle or microparticle form.**

*Key Words:* **nanoparticles; microparticles; particles; inhalation; fullerenes; $C_{60}$.**

Because of the unique physicochemical properties of nanomaterials, intense interest and enthusiasm has surrounded their use in commercial and consumer products. However, this enthusiasm has been tempered by the lack of defined information concerning the potential adverse health and environmental consequences of these nanomaterials. As nanomaterials like $C_{60}$ fullerenes continue to make their way into consumer products, humans and the environment will be increasingly exposed to these materials.

In the first reporting of the creation of man-made $C_{60}$ fullerenes, (Kroto *et al*. 1985) speculated that "Because of its stability when formed under the most violent conditions, it may be widely distributed in the universe." Indeed evidence does exist that suggest $C_{60}$ fullerenes have existed on earth for a considerable time. $C_{60}$ fullerenes occur in the environment from natural and anthropogenic sources such as volcanic eruptions, forest fires, and the combustion of carbon-based materials. In fact, environmental $C_{60}$ fullerenes have been reported in 10,000-year-old ice core samples (Murr *et al*., 2004) and dinosaur eggs (Wang *et al*., 1998). Recently air samples from urban atmospheres have been shown to contain fullerenes (Utsunomiya *et al*., 2002) demonstrating that humans are exposed to environmental fullerenes via inhalation.

One particular difficulty in studying the toxicity of $C_{60}$ fullerenes in biological systems is that they are not soluble in water (Ruoff *et al*., 1993). To overcome this difficulty, methods that utilize the organic solvent tetrahydrofuran (THF) to create water-soluble suspensions of $C_{60}$ fullerenes have been developed (Deguchi *et al*., 2001). Utilizing these water-soluble $C_{60}$ fullerene suspensions, several studies have reported that exposure to $C_{60}$ fullerenes causes toxicity in various organisms. Juvenile bass fish were reported to have increased lipid peroxidation in the brain and glutathione depletion in their gills after being placed in 0.5-ppm water-soluble $C_{60}$ fullerenes for 48 h (Oberdorster, 2004). *In vitro* studies have reported cytotoxicity in human cells exposed to water-soluble $C_{60}$ fullerenes due to the production of reactive oxygen species (Sayes *et al*., 2004) and lipid peroxidation (Sayes *et al*., 2005). Others point out that the removal of THF in the preparation of water-soluble fullerenes as described in these studies is

[1] To whom correspondence should be addressed at Battelle Toxicology Northwest, PO Box 902, Richland, WA 99354. Fax: (509)-372-4195. E-mail: bakerg@battelle.org.

incomplete (Andrievsky *et al*., 2005; Gharbi *et al*., 2005). One *in vitro* study reports that less than 10% of the suspension is residual solvent and that controls for this residual solvent did not contribute to reactive oxygen production or cell death (Sayes *et al*., 2005). In contrast to these findings are studies performed by others that report no associated toxicity or beneficial and protective effects of $C_{60}$ fullerenes (Andrievsky *et al*., 2005; Dugan *et al*., 2001; Gharbi *et al*., 2005; Mori *et al*., 2006; Scrivens *et al*., 1994). Within the scientific community, opinions are mixed regarding the toxicity and safety of $C_{60}$ fullerenes.

Given the potential for human exposures to $C_{60}$ fullerenes from the environment, that no previous inhalation toxicity study of $C_{60}$ fullerenes has been conducted and the majority of studies reporting the toxicity of $C_{60}$ fullerenes have utilized water-soluble fullerenes, we proceeded to conduct an inhalation exposure study aimed at a broad assessment of multiple *in vivo* toxicological endpoints. The objectives of this study were to (1) create stable atmospheres of nanoparticle and microparticle $C_{60}$ fullerenes without the use of water or solvents, (2) compare the toxicity of $C_{60}$ fullerenes in nanoparticle and microparticle form, and (3) determine the lung burden and toxicokinetics of nanoparticlulate and microparticulate $C_{60}$ fullerenes.

## MATERIALS AND METHODS

***Test material.*** Bulk $C_{60}$ fullerene test material (99.5% purity) was purchased from SES Research, Inc. (#600-9950, Houston, TX).

***Animals.*** Following a 1-week acclimation period, approximately 10-week-old male Fischer 344 rats (Taconic, Germantown, NY) were randomized by weight into three exposure groups: control, nanoparticle exposed (2.22 mg/m$^3$ $C_{60}$ fullerenes), and microparticle exposed (2.35 mg/m$^3$ $C_{60}$ fullerenes). Thirty-four rats were assigned to each exposure group. Rats were exposed utilizing the aerosol exposure system described below for 3 h/day, for 10 consecutive days. Within 2 h of completing the last exposure, 10 rats from each exposure group were anesthetized with 70% $CO_2$. Blood was collected from the retro-orbital sinus for hematology and serum chemistry analysis. Animals were euthanized by an intraperitoneal overdose injection of pentobarbital. A complete necropsy was performed and tissue samples were collected for histopathology. Gross anatomic examination was performed at necropsy. Brain, eyes, liver, kidneys, spleen, heart, lungs, large and small intestines, testes, epididymides, urinary bladder, lymph nodes (bronchial, mandibular, mediastinal, mesenteric), larynx (three levels), and nose (three levels) were fixed in 10% neutral buffered formalin (NBF) except eyes, which were fixed in Davidson's solution overnight and then transferred to NBF. All these tissues were embedded in paraffin, sectioned, stained with hematoxylin and eosin, and evaluated microscopically for histologic lesions by a veterinary pathologist. From an additional set of six rats per exposure group, blood and lung tissues for tissue burden analysis were collected immediately following the last exposure (day 10) and 1 (day 11), 5 (day 15), and 7 (day 17) days later.

Whole-blood samples collected in tubes containing potassium-EDTA were analyzed using a Cell Dyn 3700 (Abbot Diagnostic Systems, Abbott Park, IL) according to manufacturer's instructions to determine red blood cell count, hemoglobin, packed cell volume (PCV), mean red cell volume, mean red cell hemoglobin, mean red cell hemoglobin concentration, white blood cell count, differential white blood cell count, and platelet count. Reticulocyte counts were performed manually using the Miller disk method (Brecher and Schneiderman, 1950).

Additional blood samples were collected into serum separator tubes and allowed to clot. Serum samples were collected via centrifugation. The following parameters were determined in serum samples using a Roche Hitachi 912 System (Roche Diagnostic Corporation; Indianapolis, IN) according to manufacturer's instructions: blood urea nitrogen, creatinine, glucose, total protein, albumin, globulin, albumin to globulin ratio, sorbitol dehydrogenase (SDH), alanine aminotransferase, alkaline phosphatase, and creatine kinase (CK).

***Bronchoalveolar lavage.*** After euthanasia with pentobarbital, bronchoalveolar lavage (BAL) fluid was collected from the left lobe by lavage with phosphate-buffered saline. A total of six lavages were performed with lavage volumes of 5 ml per lavage. The first and second lavages were stored individually in collection tubes. The third through sixth lavages were pooled and stored together in a single collection tube. Retrieved fluid was kept on ice until lavages were centrifuged at ~1700 rpm for 10 min at ~4°C. After centrifugation, the cell-free supernatant from the first lavage was analyzed for lactate dehydrogenase and protein using Hitachi methodologies (Roche Hitachi 912 System, Roche Diagnostic Corp., Indianapolis, IN) and for 14 cytokines (Gro/KC, IL-18, IL-12 (p70), IL-2, monocyte chemottractant protein 1, tumor necrosis factor-α [TNF-α], IL-10, IL-6, IFN-γ, IL-5, IL-1β, IL-4, IL-1α, and granulocyte macrophage-colony stimulating factor; LINCO Research, St Charles, MO) using the Bio-Plex suspension array system (Bio-Rad, Hercules, CA). Samples that had a negative fluorescence value (below background) or had fluorescence value below the detectable range were designated as zero. Cell pellets from all six lavages were combined for cytological evaluations (viability, cell count, cell differentials). Cell differential smears were made using a Shandon Cytospin III Cell Preparation System Centrifuge (Shandon, Pittsburgh, PA) and stained with Romanowsky-type aqueous stain in a Wescor 7120 Aerospray Slide Stainer (Wescor, Inc., Logan, UT).

***Tissue burden analysis, calculated lung burdens, and deposition fractions.*** Following collection of lung tissues at necropsy, all tissues were frozen at − 70°C until preparation for analysis. Three milliliters of 0.1M magnesium perchlorate and 5.0 ml of toluene were added to each tissue sample. Lung tissue was homogenized using an electric tissue homogenizer; whole blood did not require homogenization. The samples were vortexed for a minimum of 180 min and centrifuged until several milliliters of toluene could be decanted off. The toluene extract was filtered using a 0.45-μm PTFE syringe filter to remove any suspended particulates and subjected to HPLC analysis.

Total $C_{60}$ burden (mass) in the lungs was calculated by multiplying the measured concentration in the right lung by the total lung weight at collection. Lung clearance rates were calculated using Equation 1:

$$A(t) = A_o\left(e^{-kt}\right), \tag{1}$$

where $A(t)$ is the lung burden (micrograms $C_{60}$) 7 days after exposure, $A_o$ is the lung burden when exposures were completed, and $k$ is the lung clearance rate constant (fraction cleared per day). Lung clearance half-lives in days ($t_{½}$) were calculated from Equation 2:

$$t_{1/2} = \frac{ln\,2}{k}. \tag{2}$$

Deposition rates were calculated from lung $C_{60}$ burdens using Equation 3. The lung burden and time at terminal sacrifice and the calculated lung clearance rate constant were used to solve for the deposition rate, α (μg/day):

$$A\left(t\right) = \frac{\alpha}{k}\left(1 - e^{-kt}\right). \tag{3}$$

In Equation 3, $A(t)$ is the lung burden (micrograms $C_{60}$) at time $t$ ($t = 10$ days on study), α is the amount of $C_{60}$ deposited (micrograms/day), and $k$ is the first-order clearance rate constant derived from Equation 1. Steady-state or equilibrium lung burdens ($A_e$, micrograms $C_{60}$) were calculated according to Equation 4:

$$A_e = \frac{\alpha}{k}. \quad (4)$$

Deposition fractions of $C_{60}$ fullerenes were calculated by dividing the $C_{60}$ fullerene lung burden by the total amount of $C_{60}$ fullerenes contained in the volume of air that would have been inhaled over the duration of the exposures assuming a minute volume of 140 ml/min for young Fischer 344 rats (Whalan *et al*., 2006). These calculations did not take into consideration any elimination of $C_{60}$ fullerenes from the lungs.

***Exposure system.*** The exposure system used to expose rats to $C_{60}$ aerosols has been previously described (Gupta *et al*., 2007). Briefly, bulk $C_{60}$ fullerene material was carefully milled in a small steel ball mill (Wig-L-Bug Amalgamtor, Cresent Manufacturing Corporation, Lyons, IL) for approximately 2 min. The milled $C_{60}$ fullerene material was suspended in a nitrogen gas stream using a rotary dust feed device (Battelle Toxicology Northwest, Richland, WA). The aerosol output was directed to a particle attrition chamber to reduce particle size. For nanoparticle exposures, output from the particle attrition chamber was directed to a quartz tube inside a furnace held at 550°C that flash vaporized the $C_{60}$ material. The furnace tube was designed to allow the introduction of additional compressed nitrogen to rapidly cool the vaporized material, causing particle condensation and accelerating the particles exiting from the tube. The output of the furnace tube was further diluted with compressed air to increase oxygen levels to $\geq$ 19.5% and was delivered to a Battelle designed nose-only exposure unit that has been previously described (Cannon *et al*., 1983). For the microparticle exposures, the only change made to this system was that the furnace tube was removed and replaced with a section of stainless steel tubing that was not heated.

Prior to initiating animal exposures, generated $C_{60}$ aerosol atmospheres were sampled from the exposure unit nose port and characterized by HPLC, XRD, and scanning laser Raman spectroscopy. During the rat exposures, exposure concentrations were determined by collecting aerosol samples on filters from representative exposure nose ports for gravimetric and HPLC analysis. For nanoparticles exposures, particle size, particle number concentrations, and surface area were determined using a scanning mobility particle sizer (SMPS; TSI, Shoreview, MN). For microparticle exposures, particle sizes were determined using a Mercer-style seven-stage impactor (In-Tox, Moriarity, NM) and aerosol mass concentrations were monitored using a calibrated real-time aerosol monitor (MicroDust PRO, Casella USA, Amherst, NH). Temperature, humidity, and oxygen concentration measurements at the nose exposure port were collected using a temperature/humidity logger (Digi-Sense, Barrington, IL) and a GT101 oxygen sensor (Gastek Inc., Newark, CA).

***HPLC analysis.*** Standards for HPLC filter analysis were prepared by weighing a known amount of bulk $C_{60}$ fullerenes into a vial containing a filter blank used for collecting aerosol samples (Pall Corporation, East Hills, NY). Ten milliliters of toluene was added to the bulk $C_{60}$ and filter samples and were dissolved by sonication for 45 min, followed by 15 min of agitation on an orbital shaker, before loading onto the chromatograph.

Standards for determining $C_{60}$ fullerene concentration in tissue samples were prepared by weighing a known amount of bulk $C_{60}$ fullerenes into a tube containing specific tissue samples from naive rats. These standards were processed as described above in the tissue burden analysis. Detection of $C_{60}$ in filter and tissue samples was performed using an Agilent 1100 HPLC equipped with an Agilent 1100 Variable Wavelength Detector. The detector was configured at a wavelength of 330 nm. The isocratic separation method injected 5 µl of toluene extract onto a Cosmosil BuckyPrep Analytical Column (SES Research, Houston, TX) with toluene as the mobile phase. The flow rate for the mobile phase was set at 1 ml/min with a run time of 20 min; retention time for the $C_{60}$ was approximately 8 min. The limit of detection for $C_{60}$ using HPLC analysis was 50 ng/ml.

***X-ray diffraction.*** Samples of the bulk $C_{60}$ test material and $C_{60}$ aerosol samples collected on filters were analyzed on a Siemens D5000 Θ/Θ diffractometer (Bruker AXS, Inc., Madison, WI) using Cu radiation at 40 kV/30 mA. Scans were run over the range of 5° to 80° with a step size of 0.02°. The count time for the samples was 10 s for the bulk powder and 35 s for the filter samples. The slits were 1 mm (incident), 1 mm (antiscatter), and 0.15 mm (detector). A scintillation detector was used for analysis. Phase identification was accomplished by matching the peak positions and intensities with those listed in the Powder Diffraction File (PDF) published by the International Centre for Diffraction Data (Newtown Square, PA).

As a further test of phase purity, Rietveld refinement was performed using a Lorentzian peak profile using Jade version 7.5 software (Materials Data Inc., Livermore, CA). The refinement process consisted of a multi-round approach in which the lattice parameters, scale factor, and sample displacement were first refined. Then, the individual profile parameters were refined followed by the isotropic thermal parameters and the atomic positions of the carbon atoms.

***Scanning laser Raman spectroscopy.*** Raman spectra of the bulk $C_{60}$ test material were obtained in the backscatter configuration using a Spex Model 1877 Raman spectrometer (Spex Industries, Metuchen, NJ) equipped with a Princeton Instruments LN/CCD detector (Princeton Instruments, Trenton, NJ). The 488.0-nm line of a Coherent Innova 307 Argon Ion Laser (Coherent Radiation, Palo Alto, CA) was used for excitation. Laser power was reduced to approximately 5 mW for most measurements to prevent sample burning, using a combination of filters and beam chopping. The slit width was 400 microns, and exposure times were 500 s for most measurements. Spectra were background corrected by subtracting the spectrum of either the glass substrate (bulk chemical samples) or the filter media (aerosol samples).

***Statistics.*** Differences between the exposed groups and the control and among different exposure groups were regarded as statistically significant at the level of $p \leq 0.05$. The one-way analysis of variance was performed followed by Bartlett's test of homogeneity of variance. If the variances were homogeneous, a Dunnett's *t*-test (modified *t*-test) was performed.

## RESULTS

### *Test Material, Nanoparticle, and Microparticle Characterization*

HPLC analysis of the procured $C_{60}$ fullerene material identified one major peak on chromatograms. Comparison of the retention time with a commercially procured standard indicated the peak was $C_{60}$. The bulk fullerene material contained > 99% of $C_{60}$ based on the total peak area. An additional unidentified peak was observed, eluting immediately after $C_{60}$ with peak areas ranging from 0.5–1% of the total peak area.

HPLC analysis of $C_{60}$ fullerene nanoparticle and microparticle aerosol samples collected on filters from the nose port revealed one major peak (Fig. 1). Comparison of the retention time with a commercially procured standard indicated the peak was $C_{60}$. The filter samples contained $\geq$ 97% of $C_{60}$ based on the total peak area. An additional unidentified peak was observed, eluting immediately after $C_{60}$ with a peak area ranging from 1 to 3% of the total peak area.

X-ray diffraction analysis (Fig. 2) revealed that the only crystalline phase detected in either the procured $C_{60}$ fullerene test material, the generated $C_{60}$ fullerene nanoparticles or micron particles, was the face-centered cubic (FCC) form of $C_{60}$ with Fm-3m symmetry (SG = 225). Rietveld refinement was performed to further test the phase purity. Reitveld refinement of the crystalline component in filter samples

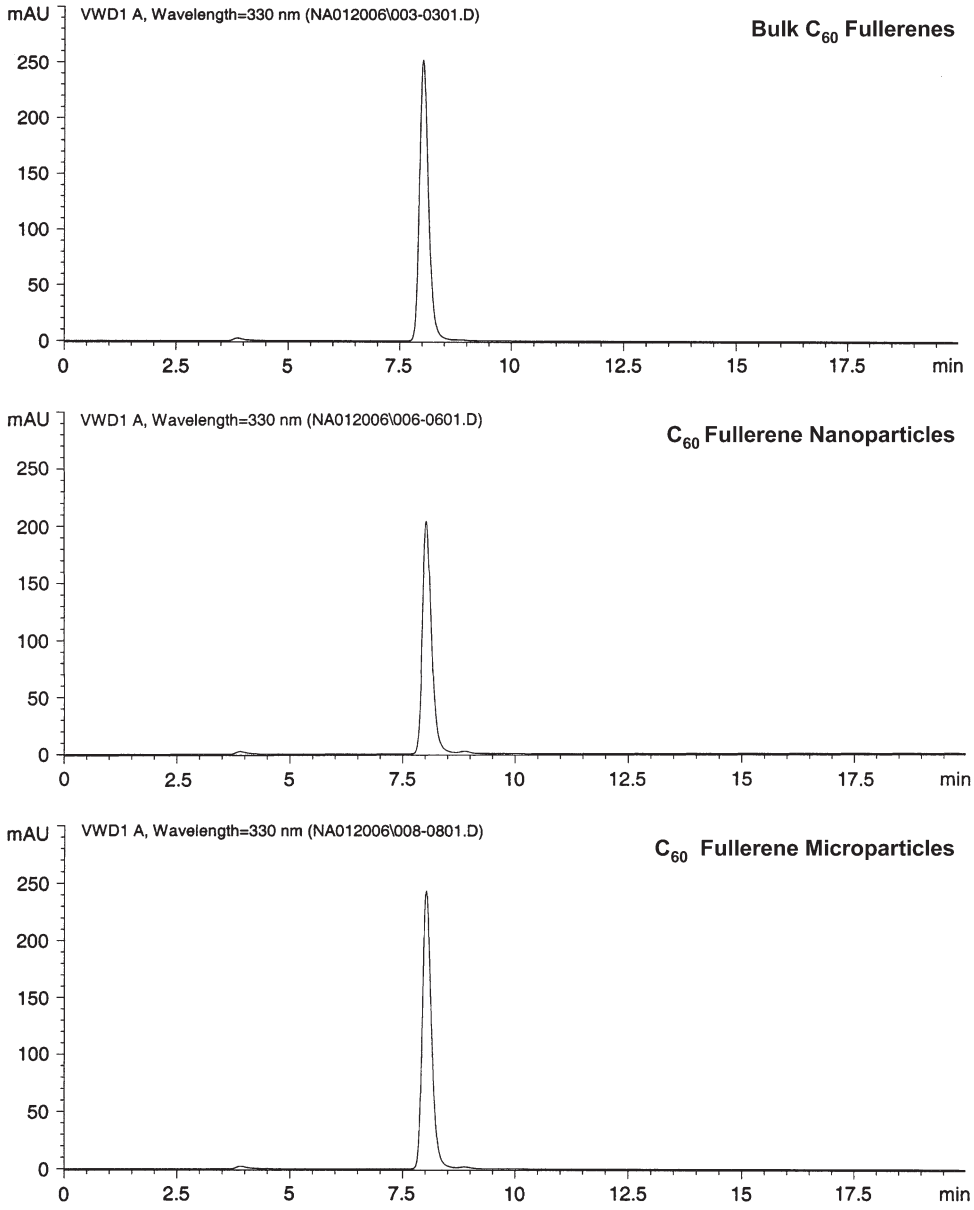


**FIG. 1.** HPLC chromatograms of $C_{60}$ fullerenes. (A) Bulk $C_{60}$ fullerene material. (B) Generated $C_{60}$ fullerene nanoparticles collected from the nose port of the nose-only exposure unit. (C) Generated $C_{60}$ fullerene microparticles collected from the nose port of the nose-only exposure unit.

confirmed that no other crystalline phases were present. All peaks obtained could be explained by the $C_{60}$ FCC structure represented by the superimposed stick pattern from the PDF. The residual plot showed no extra peaks in any of the samples, and random errors concentrated only at strong peaks. The value of the lattice parameter for $C_{60}$ fullerenes is between 14.16 and 14.166 Å. The bulk $C_{60}$ test material and filter samples had lattice parameters larger than this lattice pattern, suggesting that there may be defects in the structure (e.g., stacking faults). However, no evidence to support such defects could be found in the XRD spectra of the bulk $C_{60}$ material, or the nanoparticle, or microparticles samples collected on filters. The only polymorph of carbon detected in any of the samples was the FCC form of $C_{60}$ fullerene. The bulk $C_{60}$ fullerene test material had the largest domain size, while the filters with nanoparticles and microparticle $C_{60}$ had similar domain sizes.

Scanning laser Raman spectroscopy analysis indicated that the test material was composed primarily of $C_{60}$. The main $C_{60}$ peak in the spectrum for the nanoparticle $C_{60}$ filter (1462 per cm) was at slightly lower frequency than the bulk $C_{60}$ test material and the microparticle samples (Fig. 3). The relative intensity of the main $C_{60}$ peak (compared to the 1572 per cm peak) was also slightly smaller for nanoparticle $C_{60}$ filter, which would initially indicate slightly lower $C_{60}$ purity.

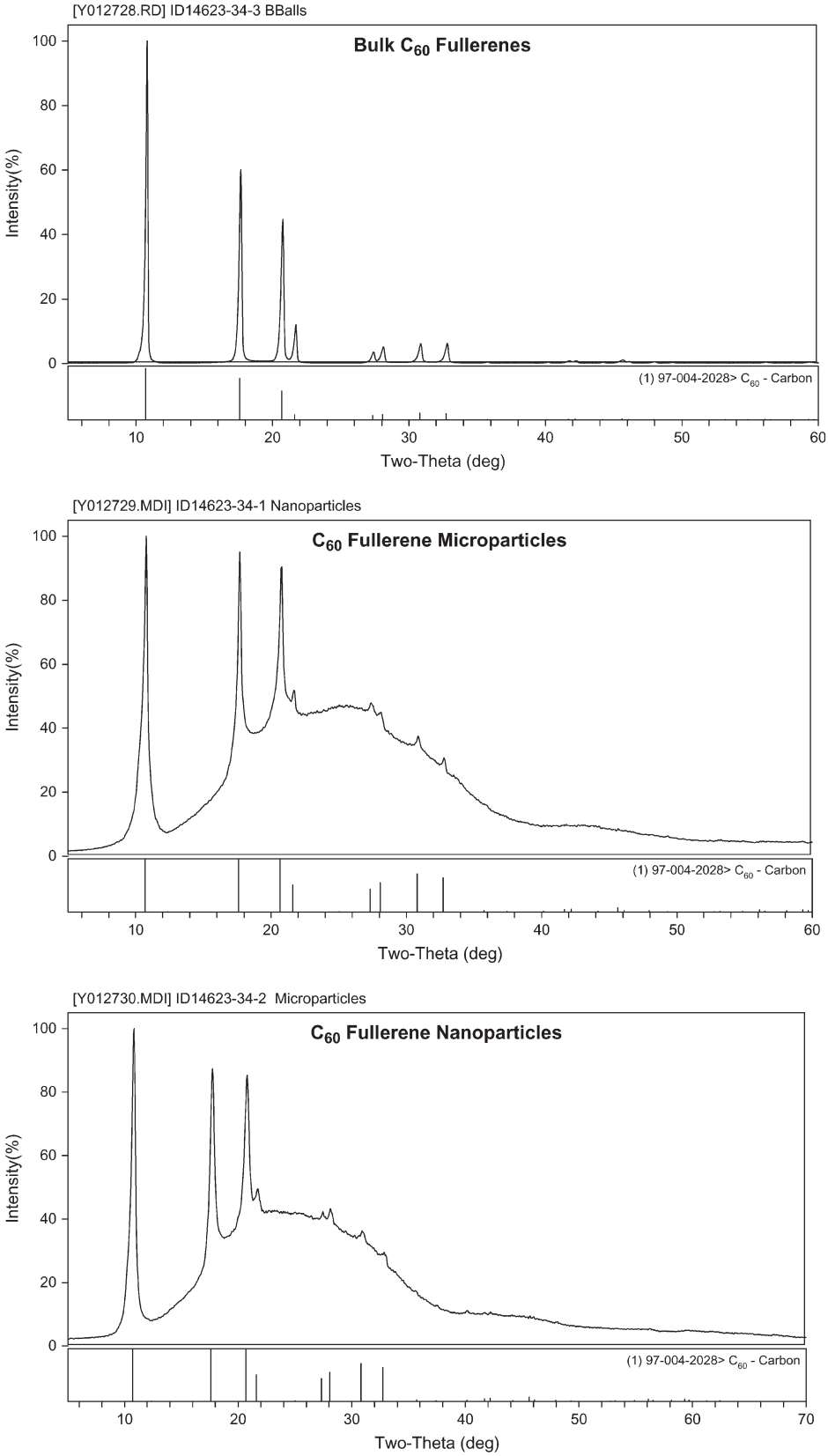


**FIG. 2.** XRD analysis of $C_{60}$ fullerenes. Bulk $C_{60}$ fullerenes were analyzed on a glass fiber filter, while nanoparticles and microparticles collected from the nose port of the nose-only exposure unit were collected on a membrane filter.

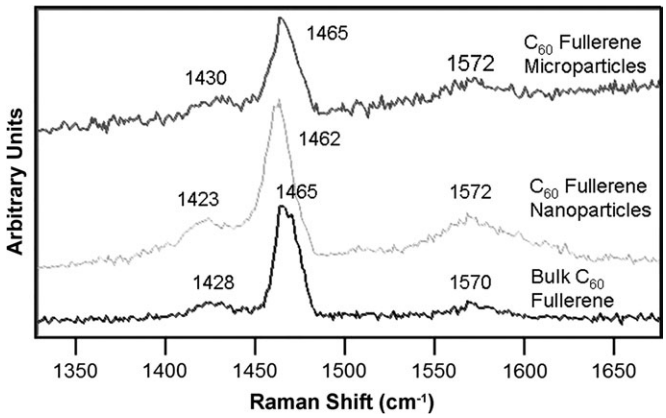


**FIG. 3.** Scanning laser Raman spectroscopy analysis of $C_{60}$ fullerene nanoparticles and microparticles collected from the nose port of the nose-only exposure unit.

However, it is suspected that the nanoparticle $C_{60}$ interacted with the laser beam, causing heating and slight decomposition of the material that resulted in the 5 per cm spectral shift. The shift of Raman bands to lower frequencies are typical when samples are heated by the laser used for Raman analysis and suggests that the nanoparticles are more reactive under the laser in air. Such increased reactivity may possibly be due to the increased surface area and/or chemical reactivity of the freshly created surface on newly created nanoparticles.

In summary, there were no significant differences between bulk test material and filter samples, indicating that the aerosol generating process did not chemically change the $C_{60}$ fullerene test material.

*Aerosol Characterization*

TEM images of generated $C_{60}$ fullerene nanoparticle and microparticles collected on lacey carbon-coated grids are presented in Figure 4. The generated nanoparticle $C_{60}$ fullerene aerosol had a count median diameter of 55 nm with a geometric standard deviation (GSD) of 1.48, an average mass concentration of 2.22 mg/$m^3$, and a particle concentration of $1.02 \times 10^6$ particles/$cm^3$. The $C_{60}$ fullerene microparticle aerosol had a mass median aerodynamic diameter of 0.93 μm with a GSD of 2.7 and an average mass concentration of 2.35 mg/$m^3$. Environmental parameter measurements at the exposure system nose ports were average temperature of 25.1°C, average relative humidity of 53%, and oxygen concentrations from 20.1 to 20.8%.

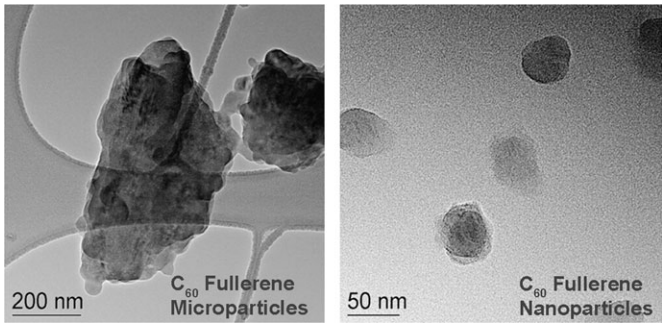


**FIG. 4.** TEM images of $C_{60}$ fullerene particles samples from the nose port of the nose-only exposure unit.

*Toxicological Findings*

During exposure, the only remarkable observation in rats exposed to both nanoparticles and microparticles was nasal and eye discharge. By the following morning, this observation had resolved and the rats were indistinguishable from controls. Body and organ weights are summarized in Table 1. Exposures to $C_{60}$ over 10 days in either nanoparticle or microparticle form did not result in any significant body or organ weights changes. No exposure-related gross anatomic lesions were seen in exposed rats. Histopathologic examination of the brain, eyes, liver, kidneys, spleen, heart, lungs, large and small intestines, testes, epididymides, urinary bladder, lymph nodes (bronchial, mandibular, mediastinal, mesenteric), larynx (three levels), and nose (three levels) did not reveal any exposure-related microscopic lesions.

Hematology and serum chemistry parameters for all exposure groups are summarized in Tables 2 and 3. There were a small number of statistically significant differences when the control group was compared to the nanoparticle- or microparticle-exposed rat groups. A statistically significant minimal decrease in red blood cells, hemoglobin, and PCV was noted in the nanoparticle-exposed group. White blood cells, monocytes, eosinophils, and platelets were minimally decreased in rats in the microparticle-exposed group. Blood glucose was significantly increased in nanoparticle-exposed

**TABLE 1**
**Absolute Organ Weights**

| | Weight in grams (mean ± SD) by exposure group | | |
|---|---|---|---|
| Parameter | Control | Nanoparticle | Microparticle |
| Body weight, before exposure | 195.6 ± 16.4 | 195.3 ± 17.3 | 193.9 ± 15.9 |
| Body weight, after exposure | 206.6 ± 17.0 | 208.0 ± 17.6 | 203.3 ± 15.4 |
| Brain | 1.79 ± 0.04 | 1.76 ± 0.05 | 1.78 ± 0.05 |
| Epididymis, right | 0.230 ± 0.063 | 0.225 ± 0.026 | 0.228 ± 0.053 |
| Heart | 0.66 ± 0.05 | 0.64 ± 0.06 | 0.62 ± 0.05 |
| Kidneys | 1.39 ± 0.10 | 1.38 ± 0.13 | 1.36 ± 0.16 |
| Liver | 7.03 ± 0.67 | 7.30 ± 0.93 | 7.16 ± 0.81 |
| Lungs | 0.70 ± 0.06 | 0.70 ± 0.04 | 0.74 ± 0.07 |
| Lymph node, bronchiolar | 0.017 ± 0.006 | 0.028 ± 0.011 | 0.032 ± 0.015 |
| Lymph node, mandibular | 0.093 ± 0.023 | 0.084 ± 0.013 | 0.109 ± 0.026 |
| Lymph node, mediastinal | 0.072 ± 0.017 | 0.070 ± 0.021 | 0.083 ± 0.023 |
| Testes, right | 1.180 ± 0.127 | 1.131 ± 0.063 | 1.153 ± 0.123 |

**TABLE 2**
**Hematology**

| Parameter | Value (mean ± SD) by exposure group | | |
|---|---|---|---|
| | Control | Nanoparticle | Microparticle[a] |
| Red blood cells ($\times 10^6$/μl) | 9.62 ± 0.25 | 9.36 ± 0.14[b] | 9.50 ± 0.23 |
| Hemoglobin (g/dl) | 16.8 ± 0.4 | 16.3 ± 0.3[b] | 16.7 ± 0.4 |
| Packed cell volume (%) | 49.1 ± 1.4 | 47.8 ± 1.0[b] | 48.4 ± 1.0 |
| Mean corpuscular volume (fl) | 51.1 ± 0.4 | 51.1 ± 0.6 | 50.9 ± 0.7 |
| Mean corpuscular hemoglobin (pg) | 17.5 ± 0.1 | 17.5 ± 0.2 | 17.5 ± 0.2 |
| Mean corpuscular hemoglobin concentration (g/dl) | 34.3 ± 0.3 | 34.2 ± 0.3 | 34.4 ± 0.3 |
| Nucleated red blood cells (per 100 white blood cell) | 0 ± 0 | 0 ± 1 | 0 ± 0 |
| Reticulocytes ($\times 10^3$/μl) | 263 ± 30 | 274 ± 57 | 247 ± 20 |
| White blood cells ($\times 10^3$/μl) | 6.12 ± 1.27 | 5.98 ± 1.20 | 4.84 ± 0.73[b] |
| Segmented neutrophils ($\times 10^3$/μl) | 1.80 ± 0.40 | 1.85 ± 0.27 | 1.53 ± 0.22 |
| Band neutrophils ($\times 10^3$/μl) | 0.00 ± 0.00 | 0.00 ± 0.00 | 0.00 ± 0.00 |
| Lymphocytes ($\times 10^3$/μl) | 4.09 ± 1.02 | 3.93 ± 1.11 | 3.22 ± 0.76 |
| Monocytes ($\times 10^3$/μl) | 0.11 ± 0.09 | 0.05 ± 0.06 | 0.03 ± 0.02[b] |
| Eosinophils ($\times 10^3$/μl) | 0.11 ± 0.05 | 0.13 ± 0.10 | 0.06 ± 0.03[b] |
| Basophils ($\times 10^3$/μl) | 0.01 ± 0.01 | 0.01 ± 0.01 | 0.01 ± 0.01 |
| Platelets ($\times 10^3$/μl) | 609 ± 67 | 580 ± 80 | 531 ± 53[b] |

[a] $N = 9$.
[b] $p \leq 0.05$ significance compared to control.

rats, while microparticle-exposed rats had increases in bile acids, CK, and decreased albumin concentration.

BAL fluid cytology and cytokine results are summarized in Tables 4 and 5, respectively. There were no statistically significant differences for the cytology data. BAL fluid protein concentrations were significantly increased in the nanoparticle-exposed group. GRO/KC and IL-18 were significantly decreased, and TNF-α and IL-1β were increased in the microparticle group. There were no significant differences in BAL fluid cytokines in the $C_{60}$ fullerene nanoparticle–exposed rats.

Some of the BAL fluid macrophages collected from nanoparticle- and microparticle-exposed rats contained globular, brown intracytoplasmic pigment (Fig. 5) which likely represents intrahistiocytic $C_{60}$. Similar accumulations were not seen in macrophages of processed histological lungs sections presumably because $C_{60}$ is soluble in the xylene utilized in tissue processing (Ruoff *et al*., 1993).

Lung burdens and elimination kinetics for $C_{60}$ are summarized in Figure 6 and Tables 6 and 7. Calculated lung burdens at the end of 10 days of exposure were 47% greater in

**TABLE 3**
**Serum Chemistry**

| Parameter | Value (mean ± SD) by exposure group | | |
|---|---|---|---|
| | Control | Nanoparticle | Microparticle |
| BUN (mg/dl) | 13 ± 2 | 15 ± 2 | 12 ± 2 |
| Glucose (mg/dl) | 142 ± 3 | 147 ± 6[a] | 151 ± 17 |
| Creatinine (mg/dl) | 0.3 ± 0.1 | 0.3 ± 0.1 | 0.3 ± 0.1 |
| Protein (g/dl) | 6.7 ± 0.4 | 6.6 ± 0.2 | 6.7 ± 0.5 |
| Albumin (g/dl) | 4.6 ± 0.1 | 4.6 ± 0.1 | 4.5 ± 0.1[a] |
| Globulin (g/dl) | 2.1 ± 0.4 | 2.1 ± 0.1 | 2.2 ± 0.5 |
| A/G ratio | 2.3 ± 0.7 | 2.2 ± 0.1 | 2.2 ± 0.3 |
| SDH (U/l) | 29.3 ± 22.6 | 14.1 ± 3.5 | 40.1 ± 23.1 |
| ALT (U/l) | 130 ± 126 | 71 ± 12 | 179 ± 93 |
| ALP (U/l) | 286 ± 59 | 328 ± 26 | 292 ± 26 |
| Bile acids (μmol/l) | 8.3 ± 2.5 | 6.5 ± 2.2 | 12.9 ± 3.2[a] |
| CK (U/l) | 439 ± 98 | 555 ± 119 | 583 ± 149[a] |

*Note*. BUN, blood urea nitrogen; A/G, albumin to globulin ratio; ALT, alanine aminotransferase; ALP, alkaline phosphatase.
[a] $p \leq 0.05$ significance compared to control.

**TABLE 4**
**BAL Fluid Cytology and Chemistry**

| Parameter | Value (mean ± SD) by exposure group | | |
|---|---|---|---|
| | Control | Nanoparticle | Microparticle |
| Total cell count (per μl) | 885 ± 267 | 904 ± 283 | 730 ± 252 |
| % Dead | 4.0 ± 1.2 | 5.0 ± 4.8 | 5.4 ± 3.2 |
| PAMs (per μl) | 879.4 ± 264.6 | 883.3 ± 251.3 | 724.5 ± 249.6 |
| PMNs (per μl) | 3.7 ± 5.1 | 17.8 ± 35.8 | 4.6 ± 4.3 |
| Lymphocytes (per μl) | 1.9 ± 3.4 | 2.5 ± 3.0 | 0.4 ± 0.9 |
| LDH (U/l) | 33 ± 8 | 40 ± 11 | 27 ± 7 |
| Protein (mg/dl) | 4.2 ± 1.4 | 7.9 ± 5.0[a] | 5.2 ± 3.2 |

*Note*. PAMs, pulmonary alveolar macrophages; PMNs, polymorphonuclear cells (neutrophils); LDH, lactate dehydrogenase.
[a] $p \leq 0.05$ significance compared to control.

**TABLE 5**
**BAL Fluid Cytokines**

| Parameters | Value in pg/ml (mean ± SD) by exposure group | | |
|---|---|---|---|
| | Control | Nanoparticle | Microparticle |
| Gro/KC | 135.06 ± 49.98 | 132.31 ± 61.50 | 93.83 ± 20.22[a] |
| IL-18 | 58.81 ± 12.45 | 69.34 ± 30.75 | 35.72 ± 7.73[a] |
| IL-12 (p70) | 0.00 ± 0.00 | 0.00 ± 0.00 | 0.00 ± 0.00 |
| IL-2 | 0.28 ± 0.88 | 1.06 ± 1.67 | 0.38 ± 1.20 |
| MCP-1 | 0.00 ± 0.00 | 0.00 ± 0.00 | 1.04 ± 2.13 |
| TNF-α | 0.13 ± 0.18 | 0.00 ± 0.00 | 0.47 ± 0.16[a] |
| IL-10 | 0.00 ± 0.00 | 0.00 ± 0.00 | 0.00 ± 0.00 |
| IL-6 | 0.00 ± 0.00 | 0.00 ± 0.00 | 0.02 ± 0.06 |
| IFN-γ | 0.00 ± 0.00 | 1.36 ± 3.67 | 0.00 ± 0.00 |
| IL-5 | 0.00 ± 0.00 | 0.00 ± 0.00 | 0.00 ± 0.00 |
| IL-1β | 0.13 ± 0.31 | 0.07 ± 0.17 | 0.84 ± 0.51[a] |
| IL-4 | 0.00 ± 0.00 | 0.00 ± 0.00 | 0.00 ± 0.00 |
| IL-1α | 0.00 ± 0.00 | 0.00 ± 0.00 | 0.00 ± 0.00 |
| GM-CSF | 0.00 ± 0.00 | 0.00 ± 0.00 | 0.52 ± 1.64 |

*Note*. MCP-1, monocyte chemottractant protein 1; TNF-α, tumor necrosis factor-α; GM-CSF, granulocyte macrophage-colony stimulating factor.
[a] $p \leq 0.05$ significance compared to control.

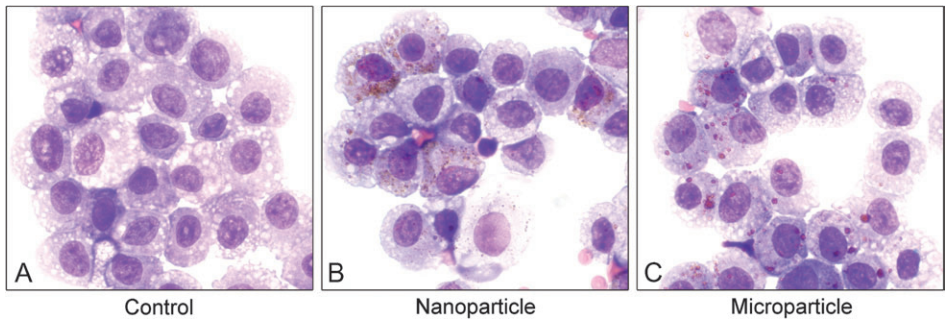


**FIG. 5.** Light microscopic images of BAL fluid cells collected from (A) control rats, (B) nanoparticle-exposed rats, and (C) microparticle-exposed rats. The red brown–colored punctuate punctate in (B) and (C) are presumed to be $C_{60}$ fullerene particles.

nanoparticle-exposed rats compared to microparticle-exposed rats. The half-life for $C_{60}$ nanoparticles in the lung was 26 days for nanoparticles and 29 days for microparticles. $C_{60}$ fullerenes were not detected in whole blood.

The calculated deposition fraction for the $C_{60}$ fullerene nanoparticle–exposed rats was 14.1% compared to 9.3% for microparticle-exposed rats. Based on the calculated difference in deposition fractions, 50% more $C_{60}$ fullerene was deposited in nanoparticle-exposed rats compared to the microparticle-exposed rats.

## DISCUSSION

We have completed the first inhalation toxicity and lung burden study of $C_{60}$ fullerene nanoparticles and microparticles. Due to the limited amount of information available on the toxicity of $C_{60}$ fullerenes, particularly in mammalian species, we chose to examine an extensive collection of toxicological endpoints to assess $C_{60}$ fullerene toxicity. In contrast to other toxicity studies of $C_{60}$ fullerene nanoparticles, our technical approach did not require the $C_{60}$ fullerene material to be water soluble eliminating the need for solvents. Throughout the aerosol generation process, the $C_{60}$ fullerene test material remained dry. Aerosol samples were collected from the nose port of the exposure unit. These samples were subjected to extensive chemical and physical characterization and compared to the procured $C_{60}$ fullerene test material. HPLC, XRD, and scanning laser Raman spectroscopy results cumulatively indicate that no chemical modification occurred during the aerosol generation process for either nanoparticle or microparticle $C_{60}$ fullerenes. TEM, SMPS, and cascade impactor results indicate that the particles were respirable in size.

Overall, 10 consecutive days of exposure to $C_{60}$ fullerene nanoparticles or microparticles resulted in minimal toxicity in rats. There were no significant differences in body or organ weights between the $C_{60}$ fullerene nanoparticle– or microparticle–exposed rats and the controls. Extensive hisopathological analysis did not identify any exposure-related lesions in the respiratory tract or any other tissues examined. Rats exposed to nanoparticle $C_{60}$ fullerenes had slight statistically significant decreases in red blood cells, hemoglobin, and pack cell volume. However, these differences were 3% or less compared to controls and are of uncertain toxicological significance. The hematological parameters in the microparticle-exposed rats had the most differences in hematology observations. White blood cells were significantly decreased by 21%, monocytes were decreased by 73%, eosinophils were decreased by 55%, and platelets were decreased 13% relative to controls. Although not statistically significant, the nanoparticle-exposed rats had a 55% decrease in monocytes, an 18% increase in eosinophils, and a minimal decrease in platelets relative to controls.

Blood SDH, an hepatic enzyme, was decreased in nanoparticle-exposed rats and increased in microparticle-exposed rats, while bile acids were also decreased in nanoparticle-exposed rats and increased in microparticle-exposed rats, suggesting an exposure-related hepatic effect for both nanoparticulate and micron-particulate exposures. However, no hepatic lesions were found in either exposure group. CK concentration was significantly increased in microparticle-exposed rats. This finding is particularly interesting since human epidemiological

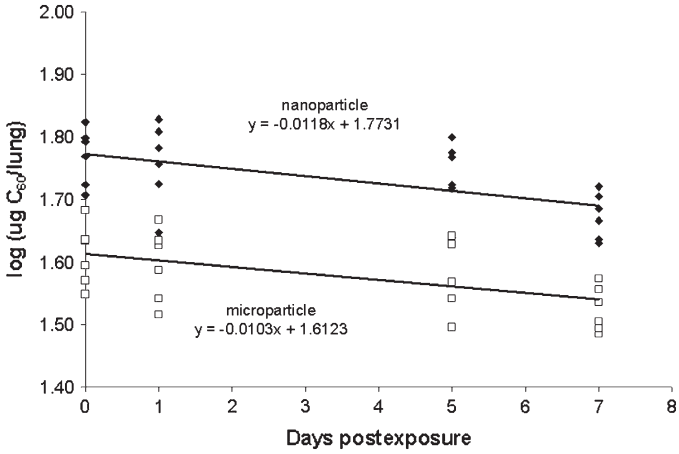


**FIG. 6.** Elimination kinetics of $C_{60}$ fullerenes from the lungs of rats following exposure to either nanoparticles of microparticles. Diamond symbols represent results from individual animals exposed to nanoparticle $C_{60}$ fullerenes. Square symbols represent results from individual animals exposed to microparticle $C_{60}$ fullerenes.

**TABLE 6**
**Lung $C_{60}$ Fullerene Burdens**

| | $C_{60}$ in μg/lung (mean ± SD) by exposure group | |
|---|---|---|
| Postexposure day | Nanoparticle | Microparticle |
| 0 | 78.89 ± 7.19 | 55.86 ± 6.32[a] |
| 1 | 75.51 ± 6.58 | 47.87 ± 8.87[a] |
| 5 | 67.63 ± 7.72 | 45.32 ± 3.18[a] |
| 7 | 58.72 ± 2.98[b] | 39.52 ± 1.08[a,b] |

[a] $p \leq 0.05$ compound to microparticle exposure group on the same postexposure day.
[b] $p \leq 0.05$ compound to days 0 and 1 within the exposure group.

studies have reported that periods of increased particulate concentrations in urban atmospheres are associated with an increased risk of myocardial infarction (Peters *et al*., 2001). As was the case for the liver, no $C_{60}$-induced lesions were observed in the hearts of either nanoparticle- or microparticle-exposed rats.

BAL fluid analysis of nanoparticle- and microparticles-exposed rats did not reveal any marked changes in BAL fluid except for increased protein concentration in $C_{60}$ fullerene nanoparticle–exposed rats. Although not statistically significant, BAL fluid polymorphonuclear (PMN) cells in nanoparticle-exposed rats were more variable than the other exposure groups. This variability was due to 2 of the 10 rats in the nanoparticle-exposed groups that had BAL fluid PMN cell counts of 114 and 39 cells/μl. The remaining eight rats had PMN cell counts that ranged from 0 to 3 cells/μl. Excluding these two rats from the nanoparticle group, the average PMN cells in the nanoparticle group are 3.0 ± 2.4 PMN cells/μl, which is comparable to the control and microparticle-exposed group averages. The significant increases in the proinflammatory cytokines, TNF-α and IL-1β, in the microparticle-exposed group BAL fluid samples are suggestive of the presence of pulmonary inflammation. However, histological examination of the lungs did not identify $C_{60}$ fullerene–induced lesions in any of the exposure groups.

As expected, the calculated lung daily deposition rate and deposition fraction of $C_{60}$ fullerene nanoparticles were 41 and 50% greater, respectively, than the microparticle-exposed rats.

**TABLE 7**
**Lung Deposition and Clearance Parameters**

| Exposure group | $k_{el}$ | $t_{1/2}$ | $C_o$ | α | $A_e$ |
|---|---|---|---|---|---|
| Nanoparticle | 0.0271 | 26 | 59.3 | 6.77 | 249.5 |
| Microparticle | 0.0237 | 29 | 41.0 | 4.60 | 194.2 |

*Note*. $k_{el}$ = lung clearance note constant; $t_{1/2}$ = half life (days); $C_o$ = lung burden at $T = 0$ (day 10) (mg); α = deposition rate constant (mg/day), $A_e$ = steady-state lung burden (mg).

It is particularly interesting that the differences in particle sizes between the two exposures only resulted in a 3-day difference in $C_{60}$ particle half-lives in the lung. These findings suggest that $C_{60}$ nanoparticle and microparticles may be eliminated from the rat lung via a common mechanism. In comparison to $C_{60}$ fullerenes, study of another carbon allotrope, carbon black (1.1 μm particles, 1 mg/m$^3$, 6 h/day, 5 days/week, for 13 weeks), reported a 64-day half-life in the lungs of rats (Elder *et al*., 2005). Like the present study of fullerenes, there were no histopathological findings associated with carbon black exposures at this exposure concentration. Steady-state lung burdens are not expected to be reached until rats are exposed over approximately 5 half-lives, which in the present study are approximately 130 days of exposure for nanoparticles and 145 days for microparticles. Since steady-state lung burdens were not reached during this study, it is possible that exposure-related toxicological findings will be found in longer duration studies.

The fact that we were unable to detect $C_{60}$ fullerenes in the blood does not preclude the possibility of biotransformation in the lung such that $C_{60}$ is rendered undetectable using our analytical technique. This possibility could be mitigated by the use of a carbon isotope–labeled $C_{60}$ fullerene in the aerosol generation system. Presently, this approach is not feasible for studies such as ours due to the lack of isotope-labeled fullerenes in sufficient amounts to conduct controlled aerosol exposures. Similar studies have used $^{13}C$ isotope–labeled carbon nanoparticle in a whole-body exposure chamber at 180 μg/m$^3$ (22 nm) for 6 h (Oberdorster *et al*., 2002). Twenty-four hours after terminating exposure, no significant changes in lung $^{13}C$ were observed, $^{13}C$ was found in the liver but not in the heart, brain, or kidney. It was unclear whether the $^{13}C$ in the liver was translocated via the pulmonary circulation or was cleared from the lung via the muco-ciliary escalator, swallowed, and absorbed from the digestive tract into the splanchnic circulation and delivered to the liver.

The nanoparticle exposure concentration tested in this study is in excess of those expected to be found within the environment. Airborne nanoparticles (<100 nm in diameter) in urban environments have been measured at mass concentrations up to 1.58 μg/m$^3$ and particle concentrations as high as $2.9 \times 10^4$ particles/cm$^3$ (Hughes *et al*., 1998). The present study tested fullerene nanoparticle concentrations that were approximately 1400 times greater in mass concentration and 35 times greater in particle concentration. Another study of carbon nanotubes in the environments where these materials are handled and transferred found mass concentrations as high as 53 μg/m$^3$ in the environment (Maynard *et al*., 2004). The mass concentration tested in the present study was approximately 41-fold greater in mass concentration. There are presently no reports of airborne fullerene concentrations in occupational environments for comparison to the present study. Therefore, the exposure concentration used in this study was deemed an appropriate starting point for the assessment of short-term $C_{60}$

fullerene inhalation toxicity. The toxicity that resulted from the tested exposure concentration indicates that future inhalation studies will need to test larger $C_{60}$ fullerene nanoparticle concentrations and/or perform longer duration exposures. A challenge to increasing the nanoparticle exposure concentration is that such increases in particle concentration decrease the stability of the generated particulate atmosphere. The only way to increase the mass concentration of an aerosol without changing the particle size is to increase the number of particles in the atmosphere. For example, using the particle concentration from the nanoparticle exposures in the present study and assuming a 50-nm spherical particle, the time in which the number of particles would decrease by half due to particle collision and coagulation, or particle half-life, is 10.6 min. If the particle size remains at 50 nm, increasing the aerosol mass concentration to 5 mg/m$^3$ requires a 2.25-fold increase in particle number, which reduces the particle half-life to 4.7 min and decreases the stability of the generated aerosol. This raises the question that if increasing nanoparticle concentrations above those tested in the present study generates unstable atmospheres, will such atmospheres be found within the environment?

In summary, we have conducted the first inhalation toxicity study of $C_{60}$ fullerenes comparing both nanoparticle and microparticle exposures. Minimal toxicity was observed in rats following 10 daily exposures to approximately 2 mg/m$^3$ $C_{60}$ fullerenes. Extensive characterization of the test material showed no chemical differences between the procured $C_{60}$ fullerene material and generated nanoparticles and microparticles. The pulmonary deposition rates and deposition fractions were greater for the $C_{60}$ fullerene nanoparticle–exposed group than the microparticle–exposed group, while the half-lives for $C_{60}$ were similar whether rats were exposed to nanoparticle or microparticle form of $C_{60}$ fullerenes. Based on the present findings, the question of whether exposures to $C_{60}$ fullerene nanoparticles result in greater toxicity than micron particle forms are inconclusive and will only be resolved through further longer duration inhalation studies.

## FUNDING

This work was funded in it's entirety by the Internal Research and Development Program of the Battelle Memorial Institute.

## REFERENCES

Andrievsky, G., Klochkov, V., and Derevyanchenko, L. (2005). Is the C60 fullerene molecule toxic? *Fuller. Nanotub. Carbon Nanostruct.* **13,** 363–376.

Brecher, G., and Schneiderman, M. (1950). A time-saving device for the counting of reticulocytes. *Am. J. Clin. Pathol.* **20,** 1079–1083.

Cannon, W. C., Blanton, E. F., and McDonald, K. E. (1983). The flow-past chamber: An improved nose-only exposure system for rodents. *Am. Ind. Hyg. Assoc. J.* **44,** 923–928.

Deguchi, S., Alargova, R. G., and Tsujii, K. (2001). Stable dispersions of fullerenes, C60 and C70, in water. Preparation and characterization. *Langmuir* **17,** 6013–6017.

Dugan, L. L., Lovett, E. G., Quick, K. L., Lotharius, J., Lin, T. T., and O'Malley, K. L. (2001). Fullerene-based antioxidants and neurodegenerative disorders. *Parkinsonism Relat. Disord.* **7,** 243–246.

Elder, A., Gelein, R., Finkelstein, J. N., Driscoll, K. E., Harkema, J., and Oberdorster, G. (2005). Effects of subchronically inhaled carbon black in three species. I. Retention kinetics, lung inflammation, and histopathology. *Toxicol. Sci.* **88,** 614–629.

Gharbi, N., Pressac, M., Hadchouel, M., Szwarc, H., Wilson, S. R., and Moussa, F. (2005). [60]Fullerene is a powerful antioxidant in vivo with no acute or subacute toxicity. *Nano Lett.* **5,** 2578–2585.

Gupta, A., Forsythe, W. C., Clark, M. L., Dill, J. A., and Baker, G. L. (2007). Generation of C60 nanoparticle aerosols in high mass concentrations. *J. Aerosol Sci.* **38,** 592–603.

Hughes, L. S., Cass, G. R., Gone, J., Ames, M., and Olmez, I. (1998). Physical and chemical characterization of atmospheric ultrafine particles in the Los Angeles area. *Environ. Sci. Technol.* **32,** 1153–1161.

Kroto, H. W., Heath, J. R., O'Brien, S. C., Curl, R. F., and Smalley, R. E. (1985). C60: Buckminsterfullerene. *Nature* **318,** 162–163.

Maynard, A. D., Baron, P. A., Foley, M., Shvedova, A. A., Kisin, E. R., and Castranova, V. (2004). Exposure to carbon nanotube material: Aerosol release during the handling of unrefined single-walled carbon nanotube material. *J. Toxicol. Environ. Health A* **67,** 87–107.

Mori, T., Takada, H., Ito, S., Matsubayashi, K., Miwa, N., and Sawaguchi, T. (2006). Preclinical studies on safety of fullerene upon acute oral administration and evaluation for no mutagenesis. *Toxicology* **225,** 48–54.

Murr, L. E., Esquivel, E. V., Bang, J. J., de la Rosa, G., and Gardea-Torresdey, J. L. (2004). Chemistry and nanoparticulate compositions of a 10,000 year-old ice core melt water. *Water Res.* **38,** 4282–4296.

Oberdorster, E. (2004). Manufactured nanomaterials (fullerenes, C60) induce oxidative stress in the brain of juvenile largemouth bass. *Environ. Health Perspect.* **112,** 1058–1062.

Oberdorster, G., Sharp, Z., Atudorei, V., Elder, A., Gelein, R., Lunts, A., Kreyling, W., and Cox, C. (2002). Extrapulmonary translocation of ultrafine carbon particles following whole-body inhalation exposure of rats. *J. Toxicol. Environ. Health A* **65,** 1531–1543.

Peters, A., Dockery, D. W., Muller, J. E., and Mittleman, M. A. (2001). Increased particulate air pollution and the triggering of myocardial infarction. *Circulation* **103,** 2810–2815.

Ruoff, R. S., Tse, D. S., Malhotra, R., and Lorents, D. C. (1993). Solubility of fullerene (C60) in a variety of solvents. *J. Phys. Chem.* **97,** 3379–3383.

Sayes, C. M., Fortner, J. D., Guo, W., Lyon, D., Boyd, A. M., Ausman, K. D., Tao, Y. J., Sitharaman, B., Wilson, L. J., Hughes, J. B., *et al.* (2004). The differential cytotoxicity of water-soluble fullerenes. *Nano Lett.* **4,** 1881–1887.

Sayes, C. M., Gobin, A. M., Ausman, K. D., Mendez, J., West, J. L., and Colvin, V. L. (2005). Nano-C60 cytotoxicity is due to lipid peroxidation. *Biomaterials* **26,** 7587–7595.

Scrivens, W. A., Tour, J. M., Creek, K. E., and Pirisi, L. (1994). Synthesis of 14C-labeled C60, its suspension in water, and its uptake by human keratinocytes. *J. Am. Chem. Soc.* **116,** 4517–4518.

Utsunomiya, S., Jensen, K. A., Keeler, G. J., and Ewing, R. C. (2002). Uraninite and fullerene in atmospheric particulates. *Environ. Sci. Technol.* **36,** 4943–4947.

Wang, Z. X., Li, X. P., Wang, W. M., Xu, X. J., Zi, C. T., Huang, R. B., and Zheng, L. S. (1998). Fullerenes in the fossil of dinosaur egg. *Fuller. Sci. Technol.* **6,** 715.

Whalan, J. E., Foureman, G. L., and Vandenberg, J. J. (2006). Inhalation risk assessment at the enivornmental protection agency. In *Inhalation Toxicology*, 2nd ed. (H. Salem and S. A. Katz, Eds.), pp. 3–37. CRC Press, Boca Raton, FL.